Dry Sliding Wear Behavior of Al_2O_3/SiC Particle Reinforced Aluminium Based MMCs Fabricated by Stir Casting Method

N. Altinkok[a], İ. Özsert[b] and F. Findik[c]

[a]Sakarya University, Hendek Vocational School, Department of Machine and Metal, Technologies Hendek — Sakarya, Turkey

[b]Sakarya University, Technology Faculty, Department of Machine Engineering, Esentepe-Sakarya, Turkey

[c]Sakarya University, Technology Faculty, Department of Material and Metallurgy Engineering Esentepe-Sakarya, Turkey

(Received Received October 9, 2012; in final form April 8, 2013)

Al_2O_3/SiC particulate reinforced metal matrix composites were produced by a stir casting process. The Al_2O_3/SiC powder mix was prepared by reaction of aqueous solution of aluminium sulphate, ammonium sulphate and water containing SiC particles at 1200 °C. 10 wt% of this hybrid ceramic powder with different sized SiC particles was added to a liquid matrix alloy during a mechanical stirring between solidus and liquidus under inert conditions. Dry sliding wear tests were conducted with a pin-on-disk friction and wear tester. The morphologies of the worn surfaces were examined using a scanning electron microscope to observe the wear characteristics and investigate the wear mechanism. An optical microscope was used to examine the precipitations of the hybrid ceramic reinforced metal matrix composites after wear tests at room temperature under dry conditions. It was found that hybrid and bimodal particle reinforcement decreased weight loss especially when SiC powder with larger grain size was used. Microstructural examination showed that besides occurring coarse SiC particle reinforcement, a fine alumina particle reinforcement phase was observed within the aluminium matrix (A332). The improvement in wear resistance of the hybrid ceramic reinforced metal matrix composites could be attributed to the ability of the larger SiC particles to carry a greater portion of the applied load, as well as to the function of the larger SiC particles in protecting the smaller alumina particles from being gouged out during the wear process. Furthermore, the incorporation of hybrid and bimodal particles increased hardness of the composites with respect to the composite with fully small sized particles.

DOI: 10.12693/APhysPolA.124.11

PACS: 01.60.+q, 62.20.Mk, 81.40.Pq

1. Introduction

It has been generally noted that metal matrix composites (MMCs) represent a new generation of materials with great potential due to their novel properties. Thus, they have attracted a considerable amount of attention lately due to their significant scientific, technological and commercial importance. Increasingly, MMCs are being used to replace conventional materials in many applications, especially in the aviation, transportation, electronics, and sport industries [1, 2], owing to the increasing performance requirements in these industries. Following the development of science and technology, discontinuously reinforced aluminium alloy matrix composites have become one of the focuses of research and practical applications in the structural composites field. Many researchers have focused on the contributions of different reinforcements for the tribological applications of MMCs. The effects of adding harder particles and fibers to reinforce MMCs in terms of their wear behavior were investigated. Some researchers found that the weight loss was remarkably reduced after hard particles (SiC, Al_2O_3) [3–12], fibers (Al_2O_3) [3, 13–15] or whiskers ($K_2Ti_4O_9$, $K_2O_6TiO_2$, SiC) [16–18] were added. Having superior mechanical properties, these composites can be used in high-speed rotating and reciprocating elements such as pistons, connecting rods, drive shafts, brake rotors, and cylinder bores [1].

Regarding single reinforced MMCs, Sahin [4] reported that the wear resistance of MMCs with a normal (N) orientation of fibers was higher than that with a planer random (PR) orientation of fibers in the case of single alumina fibers-reinforced aluminium–zinc–copper alloy composites for dry sliding wear. Kato [5] reported the effects of the size (5, 15, 120, and 200 μm) of SiC particles on the wear of a Ni matrix (ductile matrix). He found that the wear resistance was improved when the sizes of the particles increased from 15 to 200 μm but that the wear resistance was reduced with a 5 μm particle size. He also found that the effects of a volume fraction of approximately 10% SiC particles reduced the matrix wear by half.

Sliding wear tests on 10, 20 and 30 wt% Al_2O_3 particle-reinforced 2024 aluminium alloy composites were conducted by Kök and Özdin [6]. Their work showed that the wear resistance of the composites was significantly greater than that of the aluminium alloy alone. The resistance increased as the Al_2O_3 particle content and size increased and decreased as the sliding distance, the wear load and the abrasive grit size increased. Finally, Kök and Özdin [6] found that the effect of the Al_2O_3 particle size on the wear resistance was more significant than that of the particle content.

Hybrid-reinforced aluminium MMCs were also investigated. Belmonte et al. [7] found that the wear resis-

tance of Al_2O_3/20 vol.% SiC composites increased with the SiC grain size (ranging from 0.2 to 4.5 μm) due to the enhancement of the fracture toughness. Fu et al. [19] showed that Saffil/SiC/Al hybrid MMCs presented the best wear properties in comparison with Saffil/Al, Saffil/Al_2O_3/Al, and Saffil/SiC/Al hybrid MMCs under dry sliding wear conditions. The wear properties of the Saffil/Al MMCs were the best among them when were lubricated with liquid paraffin. Du et al. [20] reported that with an increase in the volume percentage of the reinforcement with a 1:1 constant hybrid ratio, the wear value of the composites decreased.

As for an equal volume fraction of the reinforcement phase, the wear-resisting property of Al matrix composites was superior to that of Al-matrix composites. Other researchers have focused on the high-temperature sliding wear. Rodriguez et al. [11] investigated aluminium–lithium alloys reinforced with SiC particles. The composite transition temperature was higher than that of the unreinforced alloy. Liu et al. [21] studied the high-temperature friction and wear behavior of Al_2O_3 and/or carbon short fibers. They found that the friction coefficient and the wear rate of the hybrid composites containing a fixed 12 vol.% Al_2O_3 decreased with an increase of the carbon fiber volume fraction up to 6 vol.%. In addition, the dominant wear mechanisms shifted to severe adhesion at test temperatures above the critical transition temperature.

Furthermore, compared with unreinforced metals, ceramic particle reinforced aluminium can feature a low thermal expansion, that can be tailored by varying the volume fraction and morphology of the ceramic phase [22]. The effects of the particulate reinforcement on dry sliding wear of MMCs have long been investigated by researchers and reviewed by Sannino and Rack [23]. It was noted that different types of matrix and reinforcements, together with different wear conditions, resulted in a different wear mechanism. Hence, the reinforcement plays quite different roles during sliding process, which affects the wear resistance of MMCs either beneficially or detrimentally. Therefore, optimum particle size, distribution and volume fraction are important. In addition to particle properties, matrix strength is also important. Several works have been carried out to increase matrix strength by aging the Al matrix but this is not sufficient to prevent wearing of Al matrix.

The wear and friction behavior of aluminum/silicon carbide (Al/SiC) composites have been extensively investigated [24]. In particular, SiC particulates employed to reinforce a variety of aluminum alloys show a trend of increasing wear resistance and decreasing friction coefficient in contrast to the unreinforced aluminum alloys. However, trends in friction coefficients for Al/SiC materials are reported to be inconsistent with other investigations using similar Al/SiC materials. For instance, in one report, SiC particles improved the wear resistance but also increased the friction coefficient over the unreinforced aluminum alloy [25].

Due to a lack of development for a common testing procedure, the wear and friction coefficient results can differ and thus are numerically difficult to compare from study to study. While rarely mentioned in the literature, each wear and friction experimental result from different studies is unique because of the conditions the two opposing materials were exposed to: pin-on-disk, ball-on-disk and block-on-ring. In addition, examples of varying conditions from laboratory to laboratory can be a problem; the atmospheric humidity, wear procedure employed (normal load, specimen geometry, sliding speed, sliding distance, test duration) in addition to counterface material and surface condition may have a dramatic effect on the results [26, 27].

This work investigates the dry abrasive wear and friction properties of a pin-on-disk sliding against A332 aluminum alloy and A332-Al_2O_3/SiCp composite with 10% volume fraction of different Al_2O_3/SiC particles size network reinforcement.

TABLE I

Mechanical and physical properties of Al_2O_3 and SiCp.

Material	Density [g/cm^2]	Diameter [μm]	Modulus [GPa]	HV
A332	2.7	–	91	81
Al_2O_3	2.9	≈ 3	308	1998
SiCp	3.2	2-10-20-38-45-53	409	2800
Al_2O_3/SiCp	3.05	2-10-20-38-45-53	358.5	1999

TABLE II

Chemical analysis of the A332 Al–Si alloy [28].

Element [wt%]										
Si	Cu	Mg	Fe	Ni	Zn	Mn	Pb	Ti	Sn	Al
8.5–10.5	2.0–4.0	0.5–1.5	1.2	1.0	1.0	0.5	0.2	0.2	0.1	remainder

2. Experimental

2.1. Material

Al_2O_3/SiC particulate reinforced metal matrix composites were produced by a stir casting process. The mechanical and physical properties of the metal matrix composite (MMC) properties of the MMC reinforcements are shown in Table I. The chemical composition of the A332 Al–Si alloy is shown in Table II. In the hybrid MMCs, both the reinforcing materials, Al_2O_3 and SiCp, were used at different sizes.

10 wt% hybrid ceramic powder mix was prepared by a chemical route, milled and then inserted in an Al–Si–Mg (A332) alloy in the melt condition by a stir-casting process. While SiC particles were supplied commercially, Al_2O_3 was chemically produced from aluminium sulphate. Al_2O_3/SiC powder mix was prepared by addition of SiC particle into the aqueous solution of aluminium sulphate, ammonium sulphate and water, followed by a reaction at 1200 °C. After this reaction, chemically produced α-alumina with uniformly distributed silicon carbide cake was fabricated and ball-milled to adjust the

alumina particle size before stir casting. 10 wt% of this hybrid ceramic powder with different sized SiC particles was added into the liquid matrix alloy during mechanical stirring between the solidus and liquidus under inert conditions.

The wear behaviours of the cast composites were investigated using the pin-on-disc test at room temperature with 1 m s^{-1} speed under 20 N and 40 N loads and dry conditions. Optical microscopy (Olympus BH2-UMA) was used to examine particle distribution and scanning electron microscope (SEM) (Camscan S4-8D7) combined with energy dispersive spectrometry (EDS) analysis was used to investigate polished and worn surfaces. Brinell hardening values of Al_2O_3/SiC particle aided MMCs materials were obtained by using a Wolpert Testor HT1a type machine with a 187.5 kg load and a 2.5 mm dimensional steel ball at the end of 30 s.

The length and diameter of the pin specimens were 15 mm and 5 mm, respectively. A steel counter disk was made of 42CrMo4. It was machined to a height of 7 mm and a diameter of 30 mm for all wear tests. The average roughness values of the pin and disk surfaces were measured after polishing with 700-grit sandpaper. These values were 0.21 μm and 0.12 μm, respectively. The weight loss amounts of the pin specimens and the disk due to sliding wear were measured by a precision electronic balance having an accuracy of 0.01 mg. The volume loss (V) of the films during wear was calculated according to the ASTM Standard G99 [29]. Finally, all of the test results are presented in terms of the wear rate ($mm^3/(N\,m)$). The instantaneous values of the calibrated normal (FN) and tangential (FT) forces were measured and the variation of the coefficient of friction (μ = FT/FN) as a function of sliding distance was determined.

2.2. Procedure of experiment

The wear tests were performed using a pin-on-disk friction and wear tester. Figure 1 shows the rotating steel counter disk of the pin-on-disk friction and wear tester. In this configuration the steel disk is static and the pin moves around the disk axis, see Fig. 1, both disk and pin are pressed by the applied load. The wear tests were performed in dry sliding condition at room temperature.

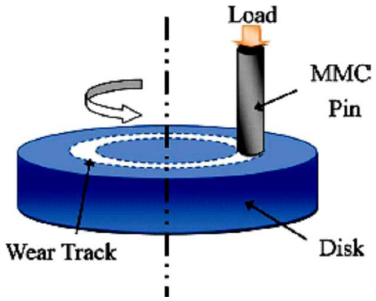

Fig. 1. Schematic view of the pin specimen and disk [3].

The testing distance is always 3600 m with a rotational velocity of 570 rpm, and the sliding diameter of the center of pin sample is 6 mm, resulting in a controlled sliding velocity of 1 m s^{-1}. The constant applied loads were 20 N and 40 N.

3. Results and discussion

Hybrid ceramic particles Al_2O_3/SiC were chemically produced by decomposition aluminium sulphate aqueous solution containing SiC particles. A slurry was prepared by mixing aluminium sulphate, $Al_2(SO_4)_3{\cdot}24H_2O$ (342 g/mol), and ammonium sulphate, $(NH_4)_2SO_4$ (132 g/mol) in water, and silicon carbide powder were added into the slurry. The resulting product was $(NH_4)_2SO_4$, $Al_2(SO_4)_3{\cdot}24H_2O$ plus SiCp after dissolving chemicals in water. This product was heated up in a ceramic crucible in the furnace. With the effect of heat, sulphate ions were volatilised and the mixture began to foam and finally Al_2O_3/SiC foam was obtained. The detailed reactions of the powder preparation have been given in Ref. [30].

SEM micrograph of this hybrid ceramic foam is in Fig. 2. According to SiC particle size and rate, the morphology of ceramic foam is changed. Smaller SiC particles cause smaller pore formation and solution containing less SiC particle results in higher porosity. This ceramic foam was milled to adjust particle size before stir casting. This hybrid ceramic powder with different SiC particle size range was added into liquid matrix alloy by the stir casting process, a 10 vol.% of hybrid ceramic particle reinforcement of these two different powder mix ceramic cake was successfully produced by the stir casting process using Al–Si–Mg alloys [30].

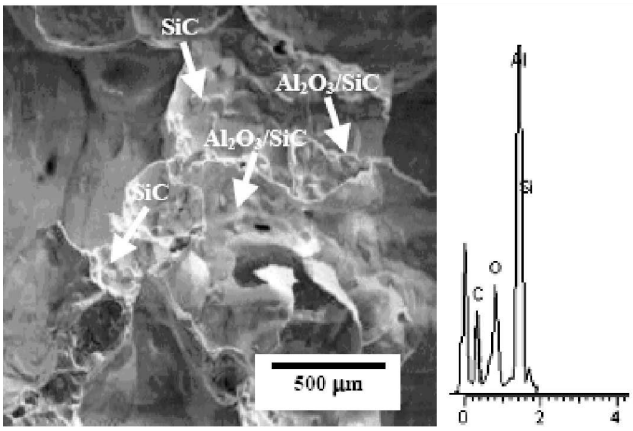

Fig. 2. (left) SEM images of porous ceramic preform Al_2O_3/SiC particle ceramic cake, (right) EDS analysis.

It is possible to control pore size by changing the amount of alumina in the cake. Since the method of alumina production results in a ceramic composite network, decreasing the alumina fraction leads to smaller volume fraction of porosity. Before alumina formation, the solution was foamed, sulphate ions were volatilized and

porous alumina formed. Therefore the rate-controlling mechanism for porosity was the shape of alumina grain grown during firing. The higher alumina was added in the system, the higher porosity was obtained. When the amount of Al sulphate was higher in the solution a higher Al_2O_3/SiCp ratio was obtained and therefore larger pores were produced (Fig. 2).

Figure 2 shows a SEM micrograph of the Al_2O_3/SiC particles, produced by the chemical route from aluminium sulphate. Al_2O_3/SiC particles present a faceted morphology. Chemically produced α-alumina with uniformly distributed silicon carbide powder mix were fabricated and milled to adjust alumina particle size.

The SEM images and EDS analysis of the foamed product made with a 50/50 Al_2O_3–SiC powder blend are shown in Fig. 2. In this figure, the high magnification of the 3D skeleton structure foam in which the cells maintain their circular section is visible. Both the cell shape and the window shape are circular. The scattered SiC particles are visible within the alumina skeleton. The EDS spectrum of the chemical compositions shows an overview of the SEM image at different regions of the sample (Fig. 2b). The SEM examination with EDS analysis was carried out on a ceramic foam surface. The presence of Al, O, Si, and C-peaks in the EDS indicates the formation of alumina and the existence of SiC as a separate phase within the analyzed area. Apart from the surface reaction between SiC and suspension or fired product, no other reaction is expected during the firing and sintering process. Therefore, this SEM image (Fig. 2a) is evidence of the successful incorporation of dual ceramic (Al_2O_3–SiC) foam.

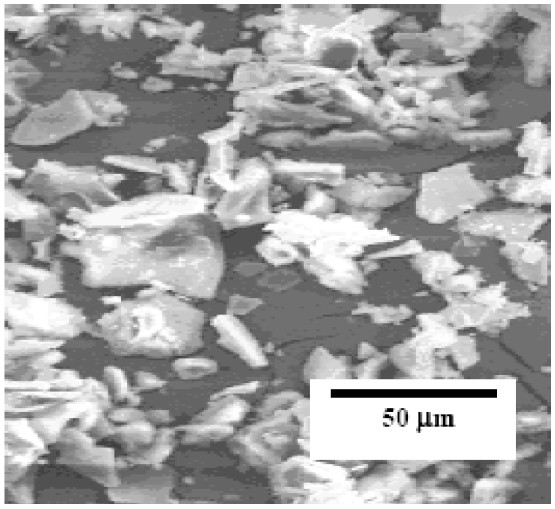

Fig. 3. SEM micrograph of milled Al_2O_3/SiC powder mix.

Figure 3 shows the SEM micrograph of the Al_2O_3/SiC particles, produced by the chemical route from aluminium sulphate. Al_2O_3/SiC particles present a faceted morphology. Chemically produced α-alumina with a uniformly distributed silicon carbide powder mix were fabricated and milled to adjust alumina particle size. At the end of the microscopic experiments, as shown in Fig. 3, larger SiC particles and smaller Al_2O_3 particles were well dispersed in the matrix and fully wetted by molten aluminium. The presences of these particles increase the mechanical properties of the composites. Silicon and magnesium in liquid aluminium increased the wettability of the matrix and assisted to the particle/matrix incorporation.

The aluminum oxide foam containing SiC particles was obtained from the firing of aluminum sulfate and ammonium sulfate aqueous solution. Figure 4 shows an X-ray analysis of this Al_2O_3–SiC ceramic foam (50–50 wt%). The analysis showed that α-alumina (corundum) was obtained after the decomposition of aluminum sulfates. Similar X-ray results were reported related to alumina production from the decomposition of aluminum sulfate and ammonium sulfate [31]. Two different SiC phases and silica were also detected. The silica comes from the oxide layer of the SiC particle surfaces. In the sintering stage, some proportion of the alumina and surface silica may form a mullite phase providing an incorporation of alumina and SiC particles. Sintering occurs between alumina/alumina and alumina/silica, which exists on the SiC particles. It is interesting to note that the Al_2O_3–SiC ceramic foam was very delicate for handling before sintering, but after sintering, the brittleness of the ceramic foam disappears and struts strength is increased as a result of improvement in bonding during sintering between Al_2O_3 and SiC particles as explained by Yamada et al. [31].

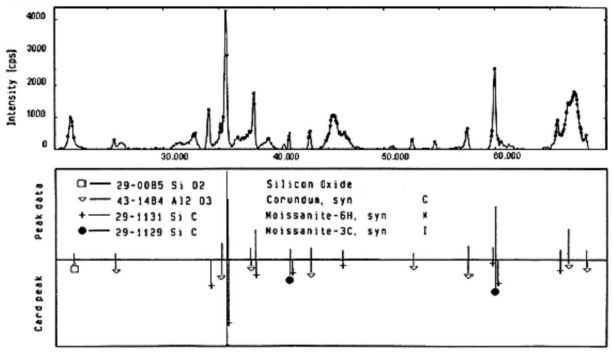

Fig. 4. X-ray diffraction pattern of the Al_2O_3–SiC ceramic foam after sintering at 1550 °C.

An optical microstructure of the stir cast composite is shown in Fig. 5. This figure reveals that large SiC particles with small Al_2O_3 particles reinforced MMC were successfully produced. It is clearly seen in Fig. 5a that the reinforcement of particles into liquid aluminium matrix alloy produced by the stir casting method has been implemented uniformly. This property of MMCs has increased the mechanical properties due to uniform distribution and the decreasing particle size. In Fig. 5b, EDS analysis is given of the SEM view of the composite polished surface containing Al_2O_3/SiC reinforcement

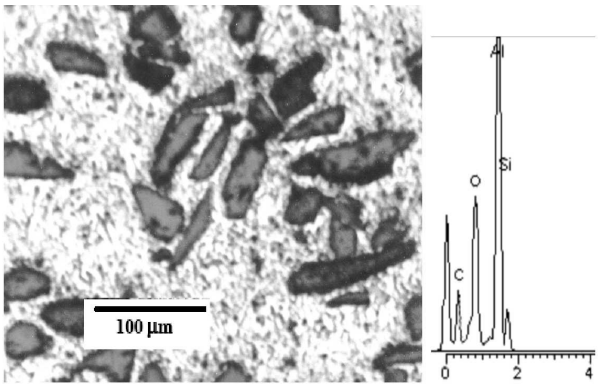

Fig. 5. (left) Polish surface of Al_2O_3/SiCp reinforced MMC optical micrograph and (right) EDS analysis.

with a different particle size produced by a stir casting process. This EDS analysis showed oxygen and carbon peaks which confirm that alumina and SiC particles are present within the composites.

3.1. Dry sliding wear behavior

Figure 5 shows optical micrographs of the sliding surfaces of the pin specimens of the hybrid MMCs with a hybrid ratio of 10 wt%. In Fig. 5a, it is easily observed that the particulates are the sliding surface of the specimen.

Figure 6 illustrates the typical A332 aluminum alloy after exposure to 20 N and 40 N loads. Along the wear track, both wear mechanisms, abrasive and adhesive wear, are visible. The magnified area of a typical wear track for the A332 alloy after subjecting it to a 20 N and 40 N load is shown in Fig. 6. As a result of the larger normal load, the soft aluminum has a greater amount of material uplift on the inner and outer circumferences of the wear track, as well as wider grooves, as compared to the 20 N loaded specimens. Both adhesive and abrasion wear are present. At a lower load, abrasion is the major wear mechanism while at higher loads adhesion is the main wear mechanism.

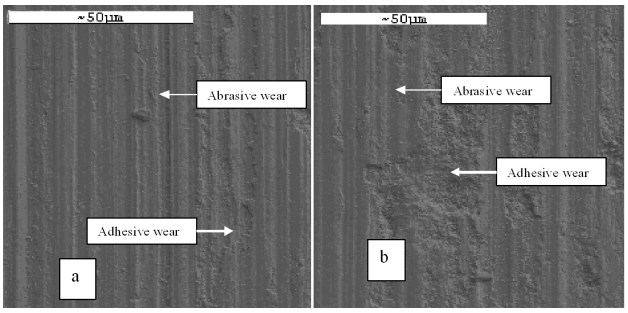

Fig. 6. SEM of the A332-20 N (a), and 40 N (b) wear surface, arrow indicates the direction of rotation.

The morphology of the worn surfaces after 3600 m of dry sliding wear presented in Fig. 6 was examined by SEM. The tribological characteristics were observed and the wear behavior was investigated. For fine particle size MMCs were easily pulled out whole from the matrix due to the particle size increased of the reinforced particles that caused a greater weight loss during dry sliding wear. This was the main cause of the considerable weight loss of the coarse particle size MMCs. From a comparison of Fig. 7a and b, the wide grooves in the worn surface of the fine particle size MMC can be observed. This indicates that the main wear mechanism was abrasive wear. In the worn surface of the fine particle size MMCs, lamination defects were observed directly and the weight loss was mostly caused by adhesive wear. The major wear mechanisms of the A332 alloy are adhesive and abrasive wears which occur at sliding speeds up to 1 m/s.

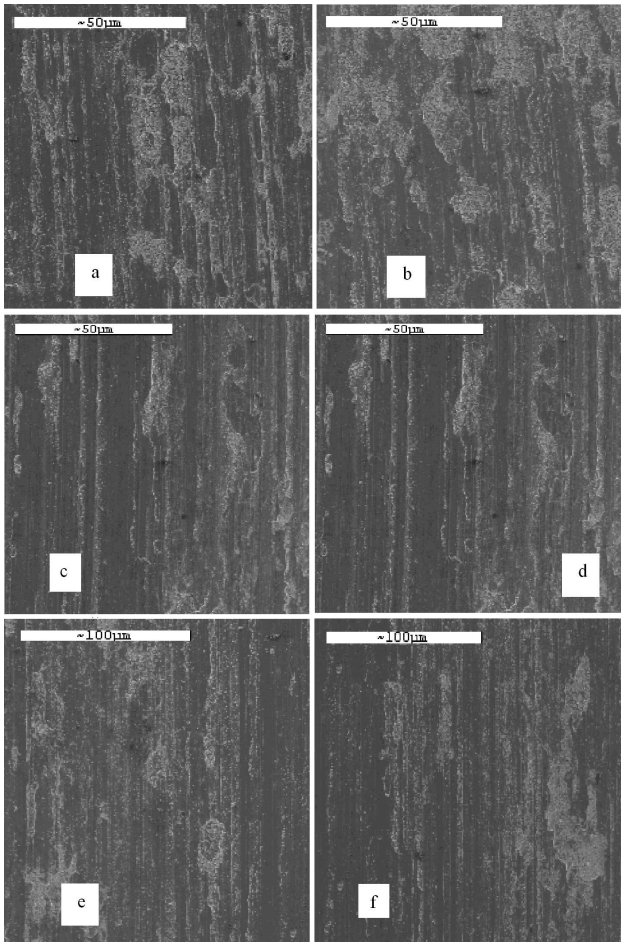

Fig. 7. SEM images of the worn surfaces of MMC specimens particle sizes: (a) 2 μm, (b) 10 μm, (c) 20 μm, (d) 38 μm, (e) 45 μm, (f) 53 μm at load 20 N.

Figure 7 illustrates the typical A332-Al_2O_3/SiCp composites after exposure to a 20 N load. Similar to the A332 alloy, the A332-Al_2O_3/SiCp composites exhibit both abrasive and adhesive wear along the wear track sliding direction. Studies on aluminum matrix composites incorporating ceramic particles have observed a sim-

ilar phenomenon: the debris particles can come loose; others may be embedded into the soft matrix while others may be crushed under the applied load forming a film between the two contacting surfaces [32].

In this work, Al_2O_3/SiC particles are shown to have beneficial effects on the tribological properties of this composite. The Al_2O_3/SiCp is shown to fracture into smaller pieces which produce wear debris particles. Other Al_2O_3/SiC particulates may prevent the penetration of the disk into the composite and thereby protect the softer aluminum from deforming increase its wear resistance. Al_2O_3/SiC particles may get crushed into powders to produce a dual effect, wear resistance and friction coefficient reduction, respectively as observed in the wear rate and friction coefficient results.

On the worn surface of the fine particle size MMC, fragmentation was easily observable, as shown in Fig. 7a. In case of the 20 μm particle size MMC under the same wear conditions, the characteristics of the worn surface were clearly different in comparison with the 38 μm particle size MMC as shown in Fig. 7b. Figure 5c and d illustrates the worn surfaces of the specimens of the MMCs, which show less surface damage. In a comparison of worn surfaces with fine particle size and coarse particle size of the MMCs, it was found that the worn surfaces became more damaged when the particle size was increased.

Additionally, the wear worsened after dry sliding wear at room temperature. A reasonable explanation for these experimental results could be the synergetic action between the hardness of the reinforcements and at room temperature at which the tests were conducted. Regarding the physical properties of the particle reinforcements, they were harder than the matrix. Hence, they could bear the load and attained the expected purpose of improving the wear behavior. However, for the hybrid MMCs, the wear rate increased with increases in the particle content. It is clear that the effect of the particles is not the same as the effect of the particles on the wear resistance. An explanation may be that the particles are distributed in a form where they act like a mat; due to the fact they have a large aspect ratio. This mat distributes the load in a large volume of the matrix, but this effect is diminished when the particle fraction increases.

The A332-Al_2O_3/SiCp composites after exposure to a 40 N load show the wear surface given in Fig. 8. The micrograph shows mixed regions of adhesive and abrasive wear in addition to some material uplift on the circumference of the wear track. Figure 8 shows the worn surfaces of the hybrid MMCs specimens with load 40 N. In Fig. 8a, although grooves were observed that were mainly caused by abrasive wear, the ploughing was relatively mild as compared to that in Fig. 8b. However, in this comparison, in the worn surface of the specimen in Fig. 8c fewer grooves and more fragmentations were observed. These were caused by adhesive wear. In the case with an increased load specimen with more severe worn surfaces were observed, as shown in Fig. 8d. It should be noted that, at room temperature, more cracks were

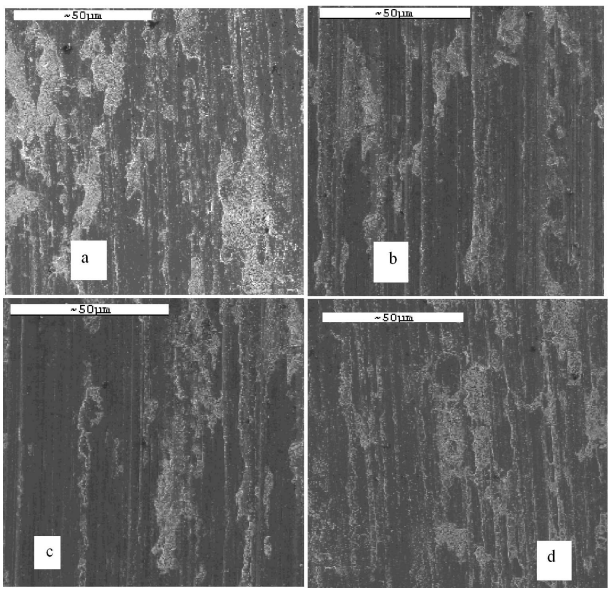

Fig. 8. SEM images of the worn surfaces of MMC specimens particle sizes: (a) 20 μm, (b) 38 μm, (c) 45 μm, (d) 53 μm at load 40 N.

observed on the worn surfaces, especially in the case of the fine size hybrid composites. However, with 10% of coarse Al_2O_3/SiCp content specimens, after the dry sliding wear, less ploughing worn surfaces were noted in both cases as shown in Fig. 8.

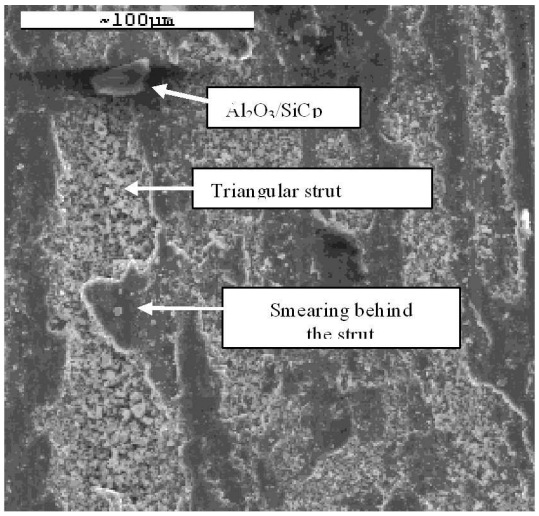

Fig. 9. A magnified view of the wear track 10 μm particle size hybrid composites at 40 N showing the cross-section outline of the triangular abraded strut. The arrow indicates the direction of rotation.

The magnified view of the wear track shows the cross-section outline of a triangular strut. Groove size decreases in width indicating less plastic deformation when the Al_2O_3/SiCp network is incorporated into the A332 alloy. Triangular strut in the wear path of the disk given

in Fig. 9 and Fig. 10, the wear grooves in the aluminum alloy appear to stop at the boundary of the abraded strut. The immediate area surrounding the strut is smooth indicating less material removal by the disk in this location. There is some smearing from the constituents of the strut material as depicted behind the strut. These observations may be the reason why the composite demonstrates improved wear and friction coefficient properties as compared to the matrix alloy.

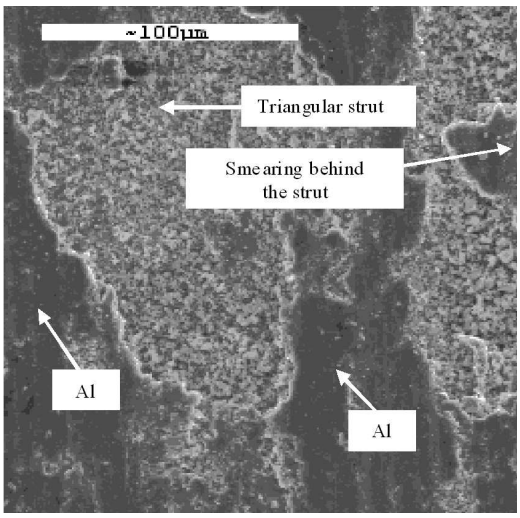

Fig. 10. The magnified view of SEM of the 20 μm particle size hybrid composites — 40 N wear surface, the arrow indicates the direction of rotation.

The microstructure of MMCs used in the experiments has been changed depending on the cooling rate of casting. This cooling rate influences the distribution of Al_2O_3/SiC particles in the casting. This effect becomes important in the case of the composite, because Al_2O_3/SiC particle distribution is affected by the growing aluminium pushed by the leading edges of growing aluminium dendrites. The cooling speed affects the particle distribution the casting process and, so, hardness resistance is affected. High cooling has caused the formation of small dendrites, and therefore, the particles have been very uniformly distributed. In addition to this homogeny distribution, with the decrease of particle size the hardness resistance of MMCs has increased.

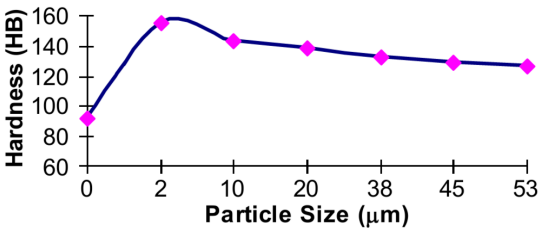

Fig. 11. Brinell hardness values of the matrix and hybrid composites.

The results of hardness experiments have been given in Fig. 11. The smallest resistance hardness values have been obtained from coarse reinforced MMCs particles. With the decrease of particle size, in spite of the increase of the porosity amount in the composites structure, the resistance and hardness values have increased [33]. Recently, in the related studies [34, 35], the decrease in reinforcement particle size, improvement in resistance and hardness have been reported as like the results given in Fig. 11. In these studies, having high resistance of reinforced thin particles MMCs had been based on the decrease of reinforcement particles and the cracking and breakings risk the situation of the high dislocation intensity and deformation.

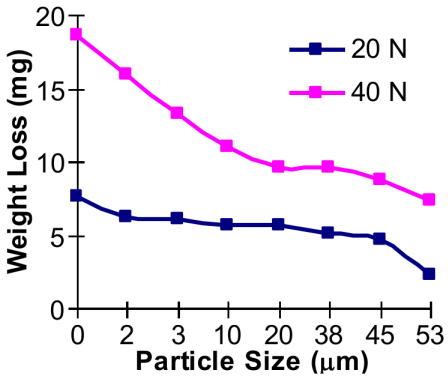

Fig. 12. Weight loss values of different Al_2O_3/SiCp MMCs.

The effects of the weight loss of the MMCs for dry sliding wear at room temperature are illustrated in Fig. 12. The wear ratio monotonically increased due to the addition and with increased Al_2O_3/SiCp size of MMCs. It was easy to determine the wear rate ratio as shown in Fig. 12. The wear losses of the Al_2O_3/SiCp composites after 3600 m sliding under 20 N, and under 40 N for comparison are shown in Fig. 12. It may be seen that although the weight loss of the alloy was higher than those of the composites, it decreased dramatically with sliding distance. Weight loss of fine particle composites was higher than the coarse of the composites. This result is similar to that reported by Salvador et al. [36] and Yılmaz and Buytoz [37].

Dry sliding wear tests of 2, 10, 20, 38, 45, 53 μm SiCp with or without alumina reinforced composites and the matrix alloy were carried out using a pin-on-disk and the results are plotted in Fig. 13. Increase in particle size decreases volume loss of composites for either monolithic or dual particle reinforcement. However, for dual and bimodal particle (Al_2O_3/SiC) reinforcement each composite showed lower weight loss than monolithic reinforcement. This means that the second fine ceramic phase strengthens the matrix and prevents matrix wear between the coarse particles as in the aged MMCs. When the abrading disk surface contacts the coarse hard particles, it is hard to fracture or to pull-out coarse par-

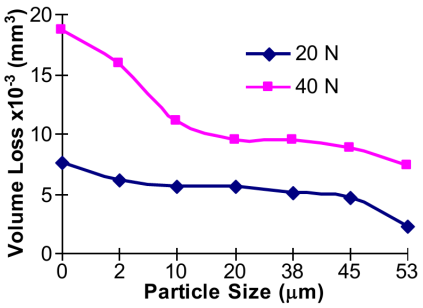

Fig. 13. Cumulative volume loss values of different Al_2O_3/SiCp MMCs.

ticles unless the matrix is worn. Since matrix hardness is increased with fine alumina particles especially for large SiCp with Al_2O_3 powder mix, reinforced composites show superior wear properties than that of monolithic SiCp reinforced composites due to good incorporation of two different particles. Those results are similar to that of Yılmaz and Buytoz [37].

3.2. Coefficient of friction

Figure 14 plots the variation of the coefficient of friction with the hybrid particle size of the MMCs at room temperature. The coefficient of friction decreased while the particle size increased. Furthermore, although the hybrid particle size had effect on the coefficient of friction, the large particle size had a greater effect on this. The coefficient of friction of the fine particle size MMCs was higher than that of the coarse particle size MMCs at room temperature. Similar coefficients of friction results have been reported for MMCs by Wang et al. [3].

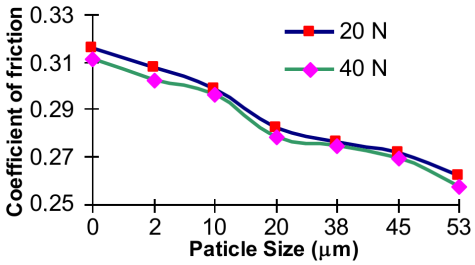

Fig. 14. Coefficient of friction of Al_2O_3/SiCp reinforced MMCs.

3.3. Strengthening mechanism

As is known, generally hard and coarse reinforcements can enhance the wear properties of composites. The results of the wear tests showed that the wear resistance increased as the Al_2O_3/SiCp size increased at room temperature. This occurred because the matrix material became softer at room temperature. The reinforcements could not resist the plastic deformation on the surfaces. Fine particle reinforcements caused more weight loss. There are two reasons for this. The first is the effect of the solid solution strengthening of the Al–Si alloy. The second phase solid solved in the matrix of the A332 Al–Si alloys were then strengthened by the precipitation of Si while the content of Mg was sufficiently high. However, the content of Mg was only 0.5–1.5 wt%, as shown in Table II. In this case, the highest solubility of Mg_2Si which was 1.85 wt% in Al–Si alloy could not be reached, despite the fact that all of the Mg was converted to Mg_2Si [32]. Therefore, during the wear test at room temperature, there was no more Mg_2Si to be solved to improve the wear properties. The reason was the effect of precipitation strengthening. As shown in Fig. 12a, reinforcements of Al_2O_3/SiCp were easily observed.

4. Conclusion

Hybrid MMCs were tested for their dry wear behaviors by a pin-on-disk friction and wear tester at room temperature. Through the above analysis and comparisons of the test results, the following can be summarized.

1. Processing variables such as holding temperature, stirring speed and the position of the impeller in the melt are among the important factors to be considered in the production of cast metal matrix composites as these have an effect on mechanical properties. These are determined by the reinforcement content, its distribution, the level of the near contact of the wetting with the matrix materials, and also the porosity content.

2. Aluminium-based metal matrix composites containing 10 vol.% of Al_2O_3/SiC particles were successfully synthesized by the stir casting route used in the present study. Uniform distribution of Al_2O_3/SiC particles in matrix alloy was successful. Fine alumina containing coarse SiCp powder mix can be produced by a chemical route. Successful particle matrix incorporation can be achieved by the stir casting process. The wear behaviors of Al_2O_3/SiC reinforced aluminium matrix composites differed from that of SiCp reinforced MMC. With hybrid particle distribution within the matrix, higher wear resistance was obtained. Fine Al_2O_3 particles hardened the matrix and decreased the wear rate since they were well distributed in the inter-particles spacing of coarse SiC particles within the aluminium matrix.

3. Wear tests showed that the wear strength of 10 vol.% Al_2O_3/SiCp hybrid ceramic powder composites decreased with increasing reinforced Al_2O_3/SiC particle size. Comparing the fine particle size MMCs with the coarse particle size MMCs were easily pulled out whole from the matrix. This was the reason for higher weight loss and volume loss of the fine particle size MMCs compared to the coarse particle size MMCs. The wear resistance of coarse particle size reinforcement MMCs reinforcement at room temperature was superior to that of the hybrid-reinforcement MMCs after dry sliding wear.

4. The wear resistance of hybrid MMCs shows a decreasing trend in MMCs cases, as the Al_2O_3/SiCp hybrid ceramic powder composites increase with increasing reinforced SiC particle size. The wear mechanisms of MMCs

with the fine Al_2O_3/SiCp were abrasive, while this was principally adhesive for hybrid MMCs with the coarse Al_2O_3/SiC particle size. Additionally, the results of the coefficient of friction of a fine hybrid particle size MMCs tested were lower than that of a coarse particle size MMC tested at room temperature.

Acknowledgments

The authors would like to thank Department of Materials Science and Engineering of Anadolu University and Sakarya University for the SEM and mechanical tests investigations.

References

[1] J.W. Kaczmar, K. Pietrzak, W. Włosiński, *J. Mater. Process. Technol.* **106**, 58 (2000).

[2] J. Barcena, J. Maudes, M. Vellvehi, X. Jorda, I. Obieta, C. Guraya, L. Bilbao, C. Jiménez, C. Merveille, J. Coleto, *Acta Astronaut.* **62**, 422 (2008).

[3] Y.Q. Wang, A.M. Afsar, J.H. Jang, K.S. Han, J.I. Song, *Wear* **268**, 863 (2010).

[4] Y. Sahin, *Wear* **223**, 173 (1998).

[5] K. Kato, *Wear* **241**, 151 (2000).

[6] M. Kök, K. Özdin, *J. Mater. Process. Technol.* **183**, 301 (2007).

[7] M. Belmonte, M.I. Nieto, M.I. Osendi, P. Miranzo, *J. Eur. Ceram. Soc.* **26**, 1273 (2006).

[8] Y. Sahin, *Mater. Des.* **24**, 95 (2003).

[9] N. Natarajan, S. Vijayarangan, I. Rajendran, *Wear* **261**, 812 (2006).

[10] S.Y. Zhang, F.P. Wang, *J. Mater. Process. Technol.* **182**, 122 (2007).

[11] J. Rodriguez, P. Poza, M.A. Garrido, A. Rico, *Wear* **262**, 292 (2007).

[12] B.S. Ünlü, *Mater. Des.* **29**, 2002 (2008).

[13] S.O. Yilmaz, *Tribol. Int.* **40**, 441 (2007).

[14] V.A. Romanova, R.R. Balokhonov, S. Schmauder, *Acta Mater.* **57**, 97 (2009).

[15] M.R. Rosenberger, E. Forlerer, C.E. Schvezov, *Wear* **266**, 356 (2009).

[16] M.W. Bai, Q.J. Xue, W.M. Liu, S.R. Yang, *Wear* **199**, 222 (1996).

[17] S.J. Kim, M.H. Cho, D.S. Lim, H. Jang, *Wear* **251**, 1484 (2001).

[18] T. Miyajima, Y. Iwai, *Wear* **255**, 606 (2003).

[19] H.H. Fu, K.S. Han, J.I. Song, *Wear* **256**, 705 (2004).

[20] Z.M. Du, J.P. Li, *J. Mater. Process. Technol.* **151**, 298 (2004).

[21] L.Yao-Hui, J. Du, S.R. Yu, W. Wang, *Wear* **256**, 275 (2004).

[22] P.K. Rohatgi, P.M. Yarandi, Y. Liu, R. Asthana, *Mater. Sci. Eng.* **147A**, 1 (1991).

[23] A.P. Sannino, H.J. Rack, *Wear* **189**, 1 (1995).

[24] R.L. Deuis, C. Subramanian, J.M. Yellup, *Compos. Sci. Technol.* **57**, 415 (1997).

[25] B. Venkataraman, G. Sundararajan, *Acta Mater.* **44**, 451 (1996).

[26] *Standard test method for wear testing with a pin-on-disk apparatus*, ASTM G99-05, American Society for Testing and Materials, West Conshohocken, PA.

[27] D. Cree, M. Pugh, *Wear* **272**, 88 (2011).

[28] M.A. Azmah Hanim, S. Chang Chung, O. Khang Chuan, *Mater. Des.* **32**, 2334 (2011).

[29] American Society of Testing and Materials, ASTM Standards, G99, ASTM, Philadelphia, 03.02; 387 (1990).

[30] N. Altinkok, A. Demir, İ. Ozsert, *Composites A* **34**, 577 (2003).

[31] Y. Yamada, K. Shimojima, M. Mabuchi, M. Nakamura, T. Asahina, T. Mukai, H. Kanahashi, K. Higashi, *Mater. Sci. Eng. A* **277**, 213 (2000).

[32] D. Cree, M. Pugh, *Wear* **272**, 88 (2011).

[33] S.-V. Kamat, M. Manoharan, *J. Compos. Mater.* **27**, 1714 (1993).

[34] R.-J. Arsenault, L. Wang, C.-R. Feng, *Acta Metall. Mater.* **39**, 47 (1991).

[35] Y. Yang, C. Cady, M.-S. Hu, P. Zok, R. Mehrabian, A.-G. Evans, *Acta Metall. Mater.* **38**, 2613 (1990).

[36] M.D. Salvador, V. Amigó, N. Martinez, D.J. Busquets, *J. Mater. Process. Technol.* **143-144**, 605 (2003).

[37] O. Yılmaz, S. Buytoz, *Composit. Sci. Technol.* **61**, 2381 (2001).